

Laminar Forced Convection of a Pseudoplastic Thermodependent Fluid in an Annular Horizontal Duct

A. Horimek^{2,3}, N. Ait Messaoudene^{1,3}, W. Aich^{1,4}, M. Aichouni¹, L. Kolsi^{1,6*}
J. Ghernaout⁵

1 Department of Mechanical Engineering, Faculty of Engineering, University of Hail, KSA

2 Mechanical Engineering Institute, Department ST, Ziane Achour University, Djelfa, Algeria

3 Hydrogen Energy Applications Laboratory, Blida University, Algeria

4 Research Unit for Materials, Energy and Renewable Energies MEER, Faculty of Science Gafsa, Tunisia

5 Department of Chemical Engineering, Faculty of Engineering, University of Hail, KSA

6 Unit of Metrology and Energy Systems, National School of Engineers, University of Monastir, Tunisia

ABSTRACT

ID # (2855)

Received: 16/10/2016

In-revised: 13/12/2016

Correspondent Author:

Lioua Kolsi

E-mail: lioua_enim@yahoo.fr

KEYWORDS

Forced convection, Pseudoplastic Fluid, Annular Duct, Thermodependency, Thermal Entrance Length.

In this work, the problem of thermal development for laminar forced convection of a pseudoplastic thermodependent fluid in a concentric annular horizontal duct is numerically addressed. Three thermal conditions are assumed: inner cylinder subjected to an imposed heat flux while the outer is insulated; then the inverse; and finally both cylinders are heated with the same heat flux densities. All computations are carried out from the entrance up to the thermal fully developed stage for a flow already developed dynamically. The study objective is to illustrate the effects of the rheological index (n), aspect ratio ($r1$), thermodependency (Pn) and heating mode on velocity profiles and Nusselt number evolution in addition to thermal entrance length. The results show an improvement in heat exchange with the shear-thinning of the fluid. The outer Nusselt decreases as $r1$ decreases while the inner one improves. Overall, the thermodependency has a similar effect to that of the shear-thinning. A very important result shows the reduction in thermal length with increasing n and/or Pn . Simple, accurate and widely valid correlations are provided for Nusselt number and thermal entrance length under different conditions.

تطوير دفق صفحي للموائع غير نيوتونية داخل أنبوب أفقي حلقي أمين نهاري تالت، و رزالي مات زين

عبد الرحمان حوريمك^{2,3}، نور الدين ايت مسعودان^{1,3}، وليد عيش^{1,4}، محمد عيشوني¹، لواء القلسي^{1,6}، جمال غرنووط⁵

1 قسم الهندسة الميكانيكية، كلية الهندسة، جامعة الحائل، المملكة العربية السعودية

2 معهد الهندسة الميكانيكية، جامعة زيان عاشور، الجلفة، الجزائر

3 مختبر تطبيقات الطاقة الهيدروجينية، جامعة البليدة، الجزائر

4 وحدة بحوث المواد والطاقة والطاقة المتجددة MEER، كلية العلوم بقفصة، تونس

5 قسم الهندسة الكيميائية، كلية الهندسة، جامعة الحائل، المملكة العربية السعودية

6 وحدة المقاييس وأنظمة الطاقة، المدرسة الوطنية للهندسة، جامعة المنستير، تونس

المُستخلص

هذا البحث هو عبارة عن دراسة عديدة لمشكلة التطور الحراري أثناء الحمل الحراري الجبري للسوائل الشبه بلاستيكية المتأثرة حرارياً داخل أنبوب أفقي حلقي مركزي. و تتناول هذه الدراسة ثلاثة وضعيات حرارية: تعرض الاسطوانة الداخلية لتدفق حراري مسلط بينما الاسطوانة الخارجية معزولة ثم العكس وأخيراً كلتا الأسطوانتين يتم تسخينهما بنفس كثافة التدفق الحراري. تم تنفيذ جميع العمليات الحسابية على أساس مرحلة متطورة بشكل تام لتدفق تم تطويره ديناميكياً. الهدف من هذه الدراسة هو توضيح الآثار المترتبة لكل من مؤشر الانسيابية (n)، نسبة الأبعاد ($r1$)، التبعية الحرارية (Pn) ووضع التدفئة على ملامح السرعة و تطور عدد نوسلت بالإضافة إلى طول المدخل الحراري. أظهرت النتائج تحسناً في تبادل الحرارة مع الترقيق القصي للسائل. كما أن عدد نوسلت الخارجي ينخفض كلما انخفضت نسبة الأبعاد في حين يرتفع عدد نوسلت الداخلي. وعموماً، فإن التبعية الحرارية لها تأثير مشابه للترقيق القصي. كما أن هناك نتيجة مهمة جداً تظهر انخفاض في طول المدخل الحراري مع زيادة مؤشر الانسيابية و/أو التبعية الحرارية. و تم أخيراً وضع ارتباطات بسيطة ودقيقة وصحيحة إلى حد كبير لعدد نوسلت وطول المدخل الحراري في وضعيات حرارية مختلفة.

رقم المسودة: (2855)

تاريخ استلام المسودة: 2016/10/16

تاريخ المسودة المعدلة: 2016/12/13

الباحث المراسل: لواء القلسي

بريد الكتروني: lioua_enim@yahoo.fr

الكلمات الدالة

الحمل الحراري الجبري، السوائل الشبه بلاستيكية، أنبوب حلقي، التبعية الحرارية، طول المدخل الحراري.

Introduction

Ducts with annular geometry are often encountered in various industrial applications: heat exchangers, nuclear reactors and oil drilling are among the areas where the annular geometry is used. The primary motivation of this study is to address food industry applications where fluids are processed in heat exchangers for sterilization by heating to proper temperatures. Thermization is provided by circulating the fluid mostly circular cross section annular geometries. This geometry offers an advantage over a simple duct by providing a larger exchange surface area for the same flow section area. In many cases, fluids used in the food industry exhibit a non-Newtonian rheological behavior with an apparent viscosity highly sensitive to temperature changes.

Duct length is a key element in heat exchanger design that should be accurately determined. Usually, full thermal development is also sought for assuring that the whole fluid is treated. Moreover, fully developed conditions allow great simplifications in mathematical modeling of the flow and have therefore been extensively studied, and numerous correlations are provided in literature for Nusselt number. Such correlations come in the form of simple formulas, with specified conditions of validity, which are much more convenient to use by design engineers. In contrast, for developing flows, correct evaluation of duct length taking into account thermal entrance length often requires numerical resolutions procedures; especially in the case of complex fluids.

Heat transfer problems for non-Newtonian fluid duct flows have received a widespread coverage in the scientific literature. For a full fully developed flow (dynamically and thermally), (Manglik and Fang, 2002) have studied the effects of the shear-thinning index (n), the radii ratio (r_1) and eccentricity (ϵ) on the velocity profile, temperature profile, Poiseuille and Nusselt number values for flow in horizontal eccentric annulus. Two thermal conditions are considered. (Hashemabadi, et al., 2005) have conducted an analytical work for a flow between two concentric cylinders, subjected to the same heat fluxes for a SPTT fluid (Phan-

Thien and Tanner, 1977). Results on the effects of radii ratio and the dimensionless elasticity on the pressure gradient and Nusselt number are provided. An analytical work treating the case of a Newtonian fluid, where viscous dissipation is taken into account, is performed in (Coelho and Pinho, 2006). Correlations of wide validity with respect to radii ratio (r_1), Brinkman number (Br) and heating mode are provided. These correlations are given with tabulated coefficients for the case of constant fluxes or temperatures. For other cases not listed, an open source Fortran code is provided online (p3357). The study is extended to the case of SPTT model (Pinho and Coelho, 2006) authors showed that in the case of imposed heat fluxes, fluid elasticity improves heat exchange; especially when viscous dissipation is taken into account. In the case of imposed temperatures, a decrease in the heat exchange is revealed at low Br . (Batra and Sudarsan, 1992) have presented a numerical study that simulates the forced convection flow of a power-law fluid in a concentric annular duct. Velocity and temperature profiles are developing simultaneously with two thermal conditions. Different radii ratios (0.2; 0.5; 0.8) and rheological indices (0.2, 0.5, 1.0, 1.2, 1.5) are considered. Results focus on the radial velocity. It is found that its amplitude decreases as n increases, and vice-versa by walls friction reductions. In addition, an increase in the mean temperature with improved local Nusselt number are observed when n decreases. (Nascimento, et al., 2002) have studied the thermal development of the flow of a Bingham (Bn) fluid inside an annular concentric duct. The dynamic profile is introduced from a previous work of the authors (Nascimento, et al., 2000). A finite integral transformation technique leading to the solution of an eigenvalues problem is used. Results report the effect of Bn , radii ratio and the mode of heating (four cases are treated) on heat transfer (Nu) along the entrance zone. It is found that the yield stress leads to an improvement in Nu ; but this effect disappears when the thermal regime is established. This is explained by the fact that the yield stress, which increases with Bn , expands the plug zone unsolicited by flow shear; thus increasing parietal velocity gradient. (Soares, et al., 2003) have studied

the thermal development for a modified Herschel-Bulkley fluid. The authors show that increase in yield stress associated with reduction of index n expands the plug-zone occupying the central area, thus improving heat exchange by increasing the parietal gradient. A comparison of Nusselt number values between Newtonian fluid flow and purely plug flow ($n \rightarrow 0$; $\tau_c \rightarrow \infty$, $u(r) = U_\infty$), shows an insignificant difference for radii ratios < 0.5 while a difference of about 11% is recorded when the radii ratio tends to 1.0. Besides, their results show that thermal length increases with yield stress and decreases with shear-thinning index. This last result is confirmed in the present work. In a recent work, (Sefid and Izadpanah, 2013) discussed for a uniform dynamic and thermal profiles at the inlet, the effects of the rheological index (n), the aspect ratio (R_i/R_e) and the heating mode on the dynamic and thermal lengths, the velocity profile, the friction coefficient, wall and mixing temperatures as well as the Nusselt number evolutions. The authors have showed a decrease of the dynamic length and friction coefficient when n decreases. The opposite occurs for thermal length and Nusselt number for the four heating modes studied. Nevertheless, it is noted that the effect of the rheological index on the thermal length is not well discussed in the work. A very comprehensive work is performed by (Monteiro, et al., 2010) for the Graetz problem of a power-law fluid flow in a concentric and eccentric annulus. It was clearly shown that Nusselt number decreases with increasing eccentricity, rheological index and radii ratio for the first case of heating (inner cylinder imposed temperature and insulated outer cylinder). This result remains valid when an imposed heat flux is supposed (Manglik and Fang, 2002). For the second case of heating (the opposite), the radii ratio parameter effect is reversed. The present work shows that this result is also obtained when a uniform flux is imposed. For fluids with non-Newtonian behavior and thermodependency, not much work is available. (Nouar and Lebouchi, 1996, Nouar, et al., 2000) have conducted numerical and experimental studies for a concentric duct, while (Ait Messaoudene et al., 2011) have conducted a numerical work for an eccentric duct. All these studies report improved heat exchange

with increasing fluid thermodependency (P_n). This improvement is mainly due to the reduction of fluid consistency K , and hence viscosity, near the heated walls. Therefore, the velocity increases in the parietal region, resulting in an improved convective exchange. Eccentricity also has a great effect, especially for strong thermodependency and/or large eccentricity; which leads to reduction of viscosity in the whole narrow part. The work of (Nouar et al., 1994) for the case of a simple circular duct gives extensive interpretations for a better understanding. Experimental fluid consistency thermodependency determination methodologies are available in (Gratão et al., 2006; Gratão et al., 2007; Bernardin et al., 2009).

The bibliographic survey also reveals the complexity of Nusselt number correlations provided in many of the cited studies. Their exploitation is made quite arduous by requiring the use of coefficients data tables or numerical codes in some cases. Accordingly, the aim of the present work is to study the problem of thermal development for the flow of a thermodependent non-Newtonian fluid in a concentric annular duct; with investigation of the effects of rheological index, radii ratio and thermodependency for three heating cases. In addition, simple and accurate correlations with wide validity span are proposed for convenient engineering computations purposes. The fluid physical properties are taken from the experimental measurements done by (Nouar, et al., 2000) even for rheological law (or thermodependency ($K = K_e \exp(-P_n \cdot \theta)$).

Definition of the problem

The laminar flow of a pseudoplastic fluid in a horizontal annular pipe is studied. Three boundary conditions are considered: 1- inner cylinder heated at constant flux while the outer cylinder is insulated; 2- outer heated cylinder and insulated inner cylinder; 3- both cylinders heated at the same heat flux. The geometry of the flow is shown in Fig.1. The rheological behavior of the fluid is described by Ostwald law: ($n \leq 1.0$) where n is the fluid rheological index. The fluid consistency K , and therefore its viscosity ($\mu_a = K \cdot \dot{\gamma}$), varies with

temperature according to the equation $K=Ke \exp(-b.T)$; where Ke is the consistency of the fluid evaluated at the entrance and b is a constant determined experimentally (Nouar, et al., 2000). Dimensional analysis of the consistency term reveals a dimensionless grouping called Pearson number (Pn) ranging from 0.0 to 16.0.

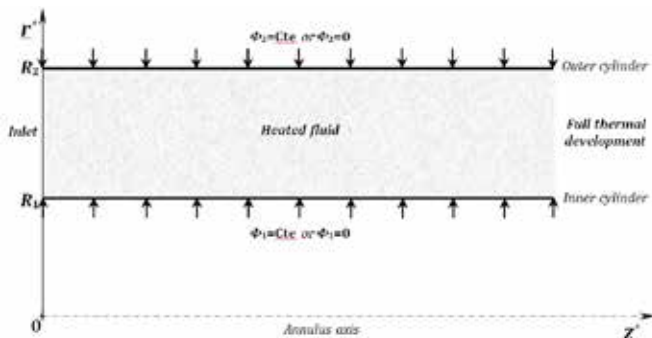


Fig. 1. Geometry of the heating annulus.

The assumptions adopted in this work are: (i) Steady state flow; (ii) Dynamically developed flow at the entrance; (iii) Negligible axial conduction; (iv) Negligible viscous dissipation; (v) Constant rheological index, thermal conductivity, specific heat and density. The ranges considered for n and Pn in the present computations are $n=[0.4; 1.0]$ and $Pn=[0.0; 10.0]$, therefore covering a wide range of fluids usually considered in practice.

Velocity Profile at the Entrance

Due to the fact that a fully developed velocity profile is assumed at the entrance, separate computations are performed for determining the velocity, pressure gradient and reference apparent viscosity. A method proposed in (Bird et al., 1987) and presented with more details in (Nouar, 1986) is adopted. In summary, the technique is based on the fact that the maximum of axial velocity corresponds to $\tau = 0$. For the annular ducts, this maximum is not on the center line between the two walls, even for a Newtonian fluid. It changes position with the aspect ratio $r1$ and the value of the rheological index n . Using the simplified axial movement equation and the rheological behavior law, two expressions of velocity in integral forms are obtained. By equalizing them at the point of maximum velocity, and using the 20 points

Gaussian integration method associated with the bisection method, one can determine the radial position of the maximum. Thereafter, the velocity profile and the pressure gradient are determined for all remaining points of the annular space easily.

The effect of the rheological index n on the velocity for $r1=0.5$ is presented in Fig.2. It is clear that axial velocity gradient close to walls (parietal velocity gradient) increases when n decreases. This is the direct cause of friction reduction by viscosity decrease. Consequently, the velocity decreases in the central areas of the flow in order to maintain the same flow rate.

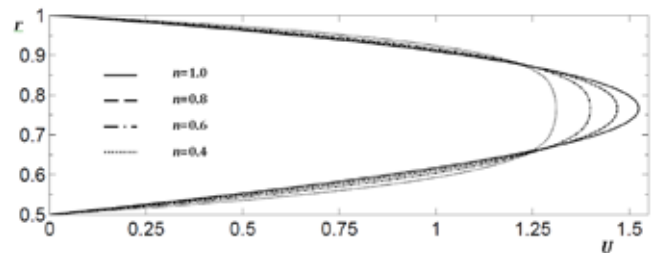


Fig. 2. Velocity profile at the entrance for various n values. $r1=0.5$.

A numerical and experimental work performed by (Ilicali and Engez, 1996) shows a good agreement between the two resolution methods. The authors present an ample literature review where it is mentioned that for the value of $r1 > 0.3$, the position of maximum velocity becomes insensitive to the value of n ; a considerable simplification is then possible by taking $n=1.0$. Other interesting results concerning this part are presented in (Nouar, 1986; Midoux, 1993).

Governing Equations

The problem of forced convection with developing temperature profile is written in cylindrical coordinates (r^*, z^*) . The equations are then non-dimensionalized using the following variables:

(1)

$$r = r^*/D_h; z = z^*/D_h; p = p^*/\rho U_d^2; U = U^*/U_d; V = V^*/U_d; \mu = \mu_a^*/\mu_a; \theta = \lambda(T - T_c)/\Phi D_h \left(\Phi = \frac{\Phi_1 + \Phi_2}{2} \right)$$

Three non-dimensional groupings appear in the equations:

(2)

$$Re = \rho U_d D_h / \mu_a ; Pe = \rho C_p U_d D_h / \lambda ; Pn = b \Phi D_h / \lambda (\text{in } \mu_a)$$

The governing equations and boundary conditions can then be written as follows:

Continuity Equation

$$(3) \quad \partial U / \partial z + \partial (rV) / \partial r = 0$$

Axial Momentum Equation

$$(4) \quad U \partial U / \partial z + V \partial U / \partial r = -\partial p / \partial z + 1/Re \partial / \partial r (r \mu_a \partial U / \partial r)$$

Energy Equation

$$(5) \quad U \partial \theta / \partial z + V \partial \theta / \partial r = 1/Pe (1/r \partial \theta / \partial r + \partial^2 \theta / \partial r^2)$$

Integral Continuity Equation

$$(6) \quad \int_{r_1/(2(1-r_1))}^{r_1/(2(1-r_1))} U.r.dr = (1+r_1)/(8(1-r_1))$$

Boundary Conditions

$$(7) \quad \begin{aligned} r = r_1/2(1-r_1) : U = V = 0 ; \partial \theta / \partial r = -1 \text{ or } \partial \theta / \partial r = 0 \\ r = 1/2(1-r_1) : U = V = 0 ; \partial \theta / \partial r = +1 \text{ or } \partial \theta / \partial r = 0 \\ z = 0 : U = U_{fd}(r) ; V = 0 ; \theta = 0 \end{aligned}$$

Numerical Procedure

Finite difference method with ADI scheme is used to discretize the equations governing the problem. A forward scheme is adopted for first derivatives and a centered scheme for second ones. Thomas’ algorithm is then used to solve the resulted tridiagonal algebraic equation system. At the entrance, the axial velocity profile, pressure gradient and reference viscosity are injected in Eq.(4) in order to compute a new velocity profile. This profile is then corrected by using the integral Eq.(6) and checked for convergence with a given error . Once the convergence is reached, the radial velocity is computed using Eq.(3) and a new pressure gradient can then be computed from Eq.(4). The corrected velocities can then be used in the energy Eq.(5) for computing the temperature field. Finally, the same procedure can be performed for the next axial step. It is noted

that when thermodependency is taken into account (Pn>0.0), the fluid consistency is updated at each axial step using (K=Ke exp(-Pn.θ)).

The integral in Eq.(6) is evaluated through the trapezoidal rule after being rearranged as Eq.(8), where ε is a correction criterion for the flow rate to be checked at each axial step:

$$(8) \quad \int_{r_1/(2(1-r_1))}^{r_1/(2(1-r_1))} U.r.dr - (1+r_1)/(8(1-r_1)) \leq \epsilon$$

It is recalled that the apparent viscosity μa, given by Ostwald’s law (μa=K.) goes to infinity when K goes to zero. This is one of the reasons for proposing more complex rheological models for this type of fluid as large values of μa (small K) generate numerical difficulties. A critical value Kc is imposed as a lower limit and the apparent viscosity is considered as fixed (frozen) at μa computed at this value for any smaller K. This technique is adopted by many authors (Nouar et al., 2000 ; Ait-Messaoudene et al., 2011; O’Donovan and Tanner, 1984). A value of Kc is adopted after a sensitivity study of the results with respect to different choices.

Mesh Size Selection

In order to select the best mesh size in terms of precision/computation time; five mesh sizes along r are tested, taking 61 elements, then 81, 101, 121 and 141. Fig. 3 shows the outer Nusselt number evolution (Nu2) for the case Φ1=Φ2. Results are strongly affected by the number of elements for coarse meshes (61 and 81); while for the remaining three, only a small change is observed with very close values of Nu2 at the fully developed zone. Similar observations are obtained for other conditions. Finally, the 101 mesh is adopted in this work.

In z direction, and in order to have accurate results, a step ΔZ=10-5 is chosen on the entire heating zone Z=0.0→0.2 (Z=z/Pe) which is largely sufficient to reach thermal development. For the case Φ1=Φ2 and r1=0.2, perturbations in the values of Nu1 are observed close to the fully developed zone; therefore, a 141 mesh with respect to r and ΔZ=10-6 are taken to overcome this problem. For the above choices, calculation time is

approximately 48 mn for most of the calculations performed. For extreme cases it slightly exceeds 15h on a Lenovo Z570 (I7, 6Go of memory).

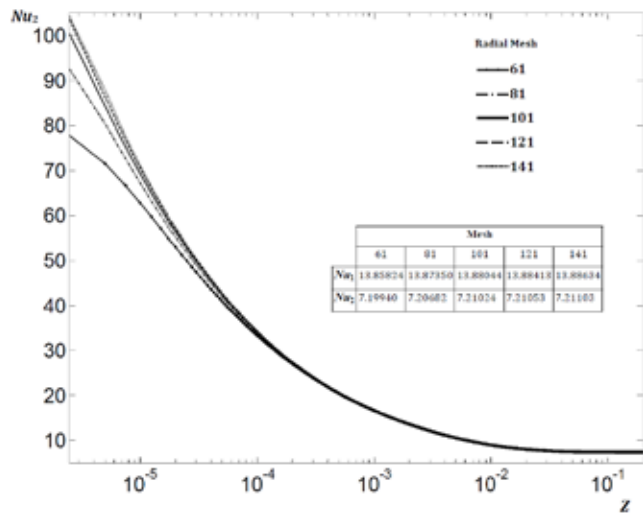


Fig. 3. Effect of the radial mesh on the outer Nusselt number evolution;
 Re=20; Pe=100; Pn=10; n=0.4; r1=0.5;
 $\Phi_1 = \Phi_2$.

Code Validation

The developed code for this work has been validated with several references (Manglik and Fang 2002; Coelho and Pinho, 2006; Sefid and Izadpanah, 2013) for many values of rheological index n and aspect ratio r1 for all the heating cases assumed. Excellent agreement between the present results and those of the selected references is shown in Table.1.

Table 1. Comparison of fully developed Nusselt number values for different n, r1 and heating modes. a: (Manglik and Fang, 2002); b: (Sefid and Izadpanah, 2013); c: (Coelho and Pinho, 2006).

Case1: $\Phi_1=0.0; \Phi_2=0.0$				Case2: $\Phi_1=0.0; \Phi_2=0.0$			
n	r ₁			n	r ₁		
	0.2	0.5	0.8		0.2	0.5	0.8
0.4	9.59853	6.31671	5.72051	5.02148	5.19886	5.38512	
	8.5551*	6.3184*	5.7824*	5.0812*	5.1921*	5.4498*	
	9.6044*	6.3505*	5.8086*	4.95046	5.10933	5.30854	
0.5	8.57091	6.28812	5.68416	4.9537*	5.0964*	5.3504*	
	8.5434*	6.2895*	5.6915*	4.90405	5.06232	5.26474	
	8.54410	6.26128	5.65442	4.8905*	5.0461*	5.2919*	
0.6	8.54410	6.26128	5.65442	4.87066	5.03427	5.23565	
	8.5253*	6.2629*	5.6617*	4.8714*	5.0163*	5.2538*	
	9.5775*	6.3008*	5.7535*	4.8827*	5.0365*	5.2365*	
0.8	8.49737	6.21503	5.61011	Case3: $\Phi_1=\Phi_2=0.0$			
	8.4806*	6.2175*	5.5932*	n	r ₁		
	9.5337*	6.2573*	5.7111*		0.2	0.5	0.8
1.0	8.44264	6.17854	5.57808	5.44918	6.41462	7.46866	
	8.4373*	6.1815*	5.5389*	5.4488*	6.4186*	7.4717*	
	8.4902*	6.2216*	5.6789*	Nu ₁	87.38724	13.10186	9.26842
8.4989*	6.1810*	5.5784*	Nu ₂	88.7086*	13.1108*	9.2718*	

Results and Discussion

To properly illustrate the effects of the various problem parameters, results are presented in two parts. The first one deals with forced convection at constant consistency (Pn= 0.0), and the second with temperature-dependent consistency (Pn> 0.0).

Forced Convection at Constant Consistency (Pn=0.0)

In Fig. 4, variation of the local Nusselt number for various values of the rheological index n is shown for the case $\Phi_1=\Phi_2$. Fig.4-a is for the outer cylinder and 4-b for the inner one. A slow decrease of Nusselt number values toward a constant fully developed value is observed. It is due to the increase in differences between the walls temperatures (θ_2 and θ_1) and the bulk temperature (θ_m). The evolutions show the significant of the index n on heat exchange that increases when n decreases. This is due to the better convective heat exchange when the velocity increases in the parietal zone, subsequent to viscosity reduction. Figures 4-a and 4-b show that the effect of n is more important for the inner cylinder. This can be explained from Fig.2 where a more important velocity increase is observed near the inner cylinder (r1=0.5).

An unexpected phenomenon is observed at the inner cylinder where Nu1 first decreases as explained above, and then increases between $Z \approx 0.01$ and $Z \approx 0.08$ before stabilizing at the fully developed value. A justification of this unexpected behavior observed can be obtained from the variation of the parietal temperatures θ_1 and θ_2 and the fluid bulk temperature θ_m (Fig.5). Near to entrance, all temperature profiles exhibit steep parietal gradients where thermal boundary layer starts. For the inner cylinder the steep slope starts to decrease just after $Z \approx 0.01$ before reaching the thermal development zone. The intermediate zone corresponds to a decrease in temperature difference between θ_1 and the θ_m ($\theta_1-\theta_m$) matching an increase in Nusselt number (small figure incorporated). This decrease is due to the fact that near the entrance, the temperature difference

between the fluid and the wall is most important; resulting in a large heat flux. Further downstream, θ_m gradually increases and the heat input from the inner cylinder slightly decreases due to the prevalence of the outer cylinder in the heating process (for equal parietal fluxes). A decrease in θ_1 variation slope ensues before arriving at the fully developed zone. It is noted that this behavior does not exist when only one of the two cylinders is heated while the other is insulated.

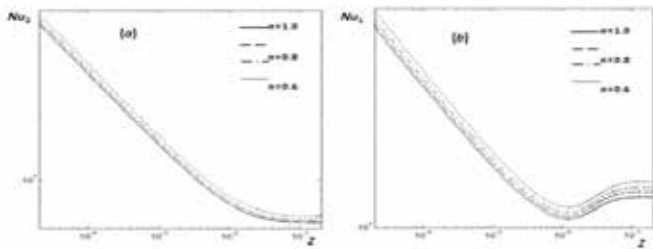


Fig. 4. Effect of the rheological index (n) on the Nusselt number evolutions. (a): Outer cylinder; (b): Inner cylinder; $Re=20$; $Pe=100$; $Pn=0.0$; $r1=0.5$; $\Phi1= \Phi2$.

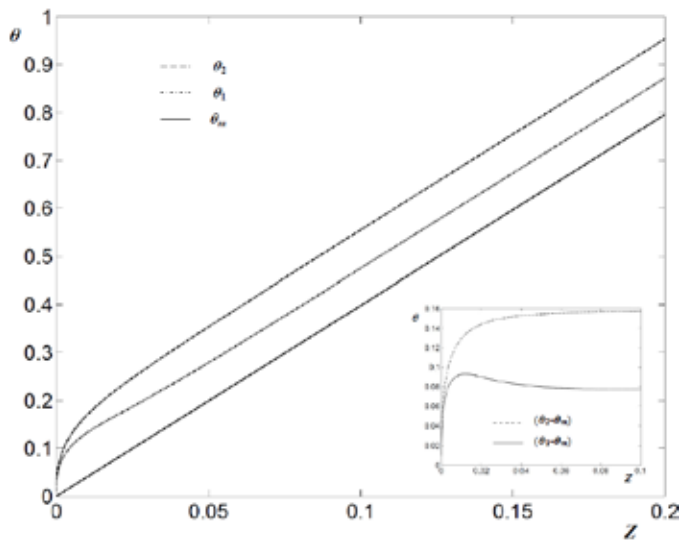


Fig. 5. Evolution of the outer cylinder (θ_2), inner cylinder (θ_1) and bulk (θ_m) temperatures along the heating zone; $Re=20$; $Pe=100$; $Pn=0.0$; $n=1.0$; $r1=0.5$; $\Phi1= \Phi2$.

The radii ratio ($r1$) also has an important effect on Nusselt number values in all three heating cases. Fig. 6-a and 6-b present its effect on Nu_2 and Nu_1

for the case $\Phi_1=\Phi_2$. A significant decrease of Nu_2 is observed with decreasing $r1$; and the inverse for Nu_1 , with a more pronounced effect. This result can be explained by the fact that when $r1$ decreases, the two cylinders are farther away from each other and therefore $(\theta_2-\theta_m)$ increases due to a decrease in θ_m ; this results in a decrease of Nu_2 . Simultaneously, the difference $(\theta_1-\theta_m)$ decreases due to the decrease in θ_1 caused by reduced incoming heat rate, in addition to the fact that θ_m value becomes closer to θ_1 as $r1$ decreases.

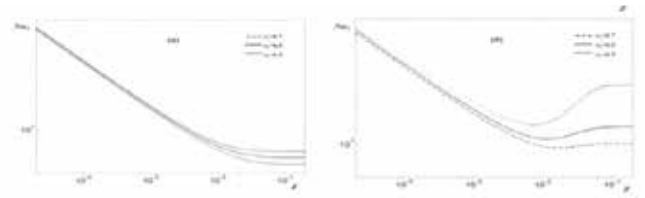


Fig. 6. Effect of the radius ratio on the evolution of: (a): Outer Nusselt (Nu_2); (b): Inner Nusselt (Nu_1); $Re=20$; $Pe=100$; $Pn=0.0$; $n=1.0$; $\Phi1= \Phi2$.

Values of the Nusselt Numbers for a Thermally Fully Developed Flow

The flow through the annular space is influenced by heating conditions, radii ratio ($r1$), in addition to rheological index (n). These parameters do not affect the shape of the evolution of the Nusselt numbers (Nu_1 ; Nu_2). But their magnitude is significantly affected over the entire entry length. Fully developed Nusselt number values in various flow configurations are very important to know. Hence, many studies are dedicated to the subject, including the case of annular geometry. Yet, lack of results is noted for the case of a heated outer cylinder and insulated inner cylinder, as well as the case of both cylinders heated for a pseudoplastic fluid. In the following part of the present work, computations are performed until full thermal development to provide values of Nu_1 and Nu_2 for different heating modes, radii ratios and values of n .

The results are correlated for ease of use in industrial applications while preserving good accuracy using the function cftool (Curve Fitting Tool) of Matlab software. For the proposed

correlations, emphasis is placed on simplicity and accuracy, in addition to clear display of the various parameters effects.

Proposed correlations: ($n=0.4 \rightarrow 1.0$; $r_1=0.2 \rightarrow 0.8$)

Case 1:
$$Nu_1 = \frac{5.80}{(5.5 + n^{0.16})(-0.83 + r_1^{0.04})} \quad (9)$$

Case 2:
$$Nu_2 = 4.97 \left(\frac{8.5 + r_1^{1.32}}{7.8 + n^{0.34}} \right) \quad (10)$$

Case 3:
$$\left. \begin{aligned} Nu_1 &= \frac{3.933}{n^{0.042} + r_1^{0.33} - 1.5} \quad (r_1 = 0.3 \rightarrow 0.8) \\ Nu_2 &= 7.468 \left(\frac{r_1^{1.15} + 1.45}{n^{0.15} + 1.22} \right) \end{aligned} \right\} \quad (11)$$

Forced convection with thermodependent consistency (Pn>0.0)

When consistency is temperature dependent, viscosity decreases near the heated walls. This phenomenon is characterized by the Pearson number ($K(\theta)=K_e \exp(-Pn.\theta)$). A high Pn indicates strong thermodependency, and vice versa. A viscosity gradient ($\mu_a=K(\theta).$) between the core zone and parietal fluid layers (heated wall (s)) of the annular is created. This generates a radial flow from the core zone towards the walls. The intensity of this flow increases with increasing Pn. Besides, the viscosity decrease close to the heated walls reduces friction; thus yielding higher flow velocities (important velocity parietal gradient). Consequently, mass conservation imposes a velocity decrease in the core zone as shown in Fig.7-a. This behavior is valid only near the entrance. Further downstream and due to the fact that the temperature of the outer wall (θ_2) increases more than that of the inner wall (θ_1), the viscosity decrease is more important close the outer wall and hence the flow velocity; especially for large Pn. As a result, a flow rearrangement is observed far from the entrance; with the maximum velocity position moving towards the hotter wall as shown in Fig.7-b. Obviously, this occurs in the case of

only one heated cylinder.

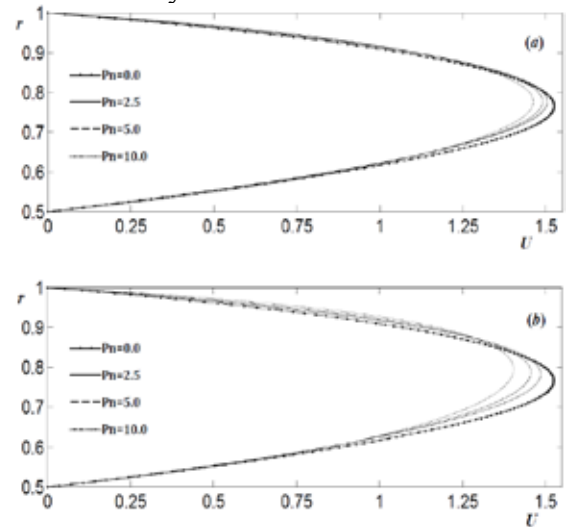
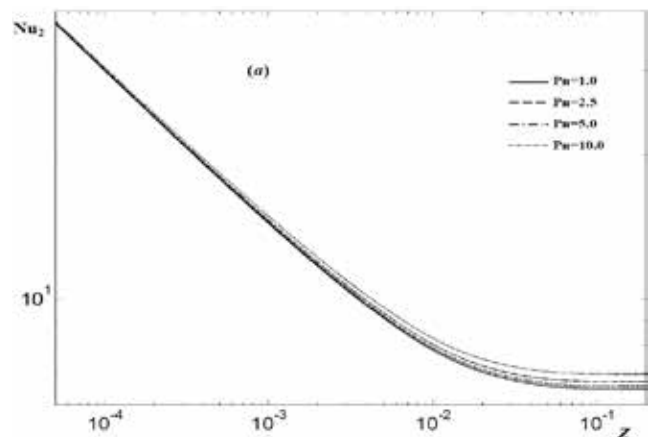


Fig. 7. Effect of thermodependency on the axial velocity. (a): $Z=0.01$; (b): $Z=0.2$; $Re=20$; $Pe=100$; $n=1.0$; $r_1=0.5$; $\Phi_1 = \Phi_2$.

In Fig.8 the variation of Nusselt number is presented for the third case of heating ($\Phi_1=\Phi_2$), where an improvement in Nu_1 and Nu_2 are observed as a result of velocity increase close to walls. Near to fully developed zone, an unexpected behavior is observed for Nu_1 , where an inversion is observed, and its value becomes smaller when Pn increases as shown in the incorporated magnified figure. This is mainly due to the rearrangement of the flow added to the secondary radial motion. At fully developed stage, values of Nu_1 and Nu_2 are calculated for different values of n and Pn for a single value of r_1 ($r_1=0.5$). The results are then correlated as performed previously for all cases.



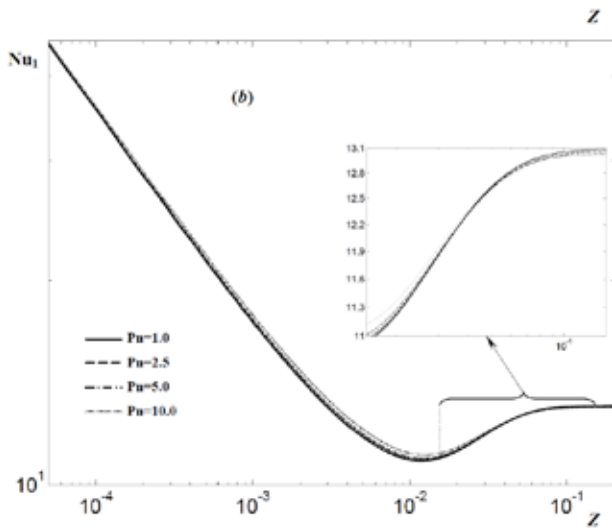


Fig. 8. Effect of the radius ratio on the evolution of: (a): Outer Nusselt (Nu_2); (b): Inner Nusselt (Nu_1); $Re=20$; $Pe=100$; $Pn=0.0$; $n=1.0$; $\Phi_1 = \Phi_2$.

Proposed correlations: ($r_1=0.5$; $n=0.4 \rightarrow 1.0$; $Pn=0.0 \rightarrow 10.0$)

Case 1: $Nu_1 = 6.1785 + 0.12(Pn^{0.89}/n^{0.6})$ (1)

Case 2: $Nu_2 = 5.0343 + 0.18(Pn^{0.9}/n^{0.47})$ (13)

Case 3: $Nu_1 = 13.1019 + 0.10(Pn^{0.09}/n^{2.79})$
 $Nu_2 = 6.4146 + 0.156(Pn^{0.53}/n^{0.5})$ (14)

Thermal Entrance Length (Zth) for Thermodependent Consistency

As detailed in the Introduction, the thermal entrance length (nearly the duct length) is of great practical importance. Hence, this part of the work deals with the effect of n and Pn on Z_{th} for the heating modes considered. For this, the case with $r_1=0.5$ and $Pe=100$ are considered.

Entrance length is considered as the distance between the inlet section and the axial position from where the Nusselt number reaches a constant value. Most authors take the axial position for which Nusselt

number reaches a given factor close to unity of the fully developed asymptotic value as a final limit. For instance, the choice of $1.05 \times Nu_{fd}$ is proposed in (Shah and London, 1971). For an imposed heat flux, (Lin et al., 2000) consider the position where $T_{wall} - T_{bulk}$ reaches 95% of its fully developed value. This choice is adopted in order to be consistent with dynamic regime development considerations. (Terhmina and Mojtabi, 1988) propose a criterion based on the idea that the temperature profile in the developing zone moves to a purely conductive shape when full development is achieved. A difference of 1% between the local Nusselt and the one at full establishment is assumed for determining the axial position of thermal development. In the present work, the position for which $Nu=1.02 \times Nu_{fd}$ is considered as the entrance length for both heating cases where only one cylinder is heated. In the third case where both cylinders are heated, the same value is adopted for Nu_2 , as it has a monotonically decreasing variation. Computations show that this position corresponds to $Nu \approx 0.95 \times Nu_{1fd}$ on the inner cylinder since Nusselt number achieves a minimum before ascending to the fully developed value as shown earlier.

Choosing $Nu=1.02 \times Nu_{fd}$ seems more appropriate, since 1.05 corresponds to a position in the zone of decreasing Nu ; still relatively far from fully developed stage. This is even more pronounced for large values of Pe , case in many industrial foods, which leads to underestimation of Z_{th} .

Then correlations for the entrance length for the three heating modes are proposed similarly to Nusselt number values. It can be seen clearly that Z_{th} decreases with increasing n and/or Pn . This result is of great importance for industrial purposes.

Proposed correlations: ($Pe=100.0$; $r_1=0.5$; $n=0.4 \rightarrow 1.0$; $Pn=0.0 \rightarrow 10.0$)

Case 1: $Z_{th}|_{z_2=0} = \frac{0.05}{(13.02 + 0.25 \times Pn^{1.30})(0.12 \times n^{0.052} - 0.053)}$ (15)

Case 2: $Z_{th}|_{z_1=0} = \frac{0.05}{(13.11 + 0.20 \times Pn^{0.55})(0.12 \times n^{0.058} - 0.054)}$ (16)

Case 3: $Z_{th}|_{z_1=z_2} = \frac{0.05}{(12.0 + 0.10 \times Pn^{1.05})(0.15 \times n^{0.072} - 0.056)}$ (17)

Conclusions

Laminar thermal development flow of a thermodependent pseudoplastic fluid in a horizontal annular duct with three heating conditions is solved numerically. Results show that:

- A gradual decrease of Nusselt number values toward fully developed values is observed for all cases of heating. Exception is observed for the inner Nusselt in the third case where it reaches a minimum in the vicinity of $Z=0.01$ before increasing until it reaches its fully developed value, due to the inner cylinder temperature slope reduction after a certain distance from the inlet;
- Improvement of the heat exchange is observed with increasing shear thinning (n), due to more significant parietal flow velocity increase;
- Decreasing the radii ratio leads to a decrease of outer Nusselt number and an increase of the inner one for the three heating conditions;
- Fluid thermodependency ($P_n > 0.0$) reduces friction near the heated walls by reducing viscosity and hence flow velocity increases. For the third heating case mode, a shift of the axial velocity' maximum towards the warmest wall occurs far from the entrance;
- An increasing improvement in heat transfer is observed when P_n increases, with an exception for Nu_1 near the full development position for the third heating mode;
- Nusselt number values by varying n , r_1 and P_n , are presented in the form of simple, accurate and widely valid correlations allowing their simple use for engineering calculations;
- Correlations reflecting the effects of n and P_n are proposed for thermal entrance length for $r_1=0.5$ and $Pe=100$. It was found that this length decreases with increasing n and P_n . This indicates that an appropriate exploitation of the fluid physical properties can yield a reduction of heat exchanger size; and therefore cost;
- Heating the two cylinders with equal flux yields a lower thermal entrance length;

- A test for non-equal fluxes may lead to further reduction; which can be combined to the previous result for heat exchangers size reduction.

Acknowledgment

The present work was undertaken within the research project (No: 0150130), funded by the Deanship of Scientific Research at the University of Hail. This is gratefully acknowledged.

References

- Horimek, A., Abed, S., and Ait-Messaoudene, N.**, Etude et corrélations pour un problème de Graetz d'un fluide pseudoplastique dans une conduite horizontale chauffée à flux constant ou à température constant, 9th days of mechanics, Algiers, Algeria, Polytechnic Military School, 2014. (proceedings)
- Manglik, R. M., and Fang, P.**, Thermal processing of viscous non-Newtonian fluids in annular ducts: effects of power-law rheology, duct eccentricity, and thermal boundary conditions. *International Journal of Heat and Mass Transfer*, vol. 45, pp. 803-814, 2002. (article)
- Hashemabadi, S. H., Etemad, S. Gh., and Thibault, J.**, Analytical Solution of Viscoelastic Fluid Flow and Heat Transfer through an Annulus. *Heat Transfer Engineering*, vol. 26, no. 2, pp. 45-49, 2005. (article)
- Phan-Thien, N., and Tanner, R. I.**, A new constitutive equation derived from network theory. *Journal of Non-Newtonian Fluid Mechanics*, 2, pp. 353-365, 1977. (article)
- Phan-Thien, N.**, A nonlinear network viscoelastic model. *Journal of Rheology*, 22, pp. 259-283, 1978. (article)

- Coelho, P.M., and Pinho, F.T.**, Fully-developed heat transfer in annuli with viscous dissipation. *International Journal of Heat and Mass Transfer*, 49, pp. 3349-3359, 2006. (article)
- Pinho, F.T. and Coelho, P.M.**, Fully-developed heat transfer in annuli for viscoelastic fluids with viscous dissipation. *Journal of Non-Newtonian Fluid Mechanics*, 138, pp. 7-21, 2006. (article)
- Batra, R.L. and Sudarsan, V.R.**, Laminar flow heat transfer in the entrance region of concentric annuli for power law fluids. *Computer Methods in Applied Mechanics and Engineering*, 95, pp. 1-16, 1992. (article)
- Nascimento, U. C. S., Macêdo, E. N. and Quaresma, J. N. N.**, Thermal entry region analysis through the finite integral transform technique in laminar flow of Bingham fluids within concentric annular ducts. *International Journal of Heat and Mass Transfer*, 45, pp. 923-929, 2002. (article)
- Nascimento, U. C. S., Macêdo, E. N., and Quaresma, J. N. N.**, Solution for the thermal entry region in laminar flow of Bingham plastics within annular ducts via integral transformation. *Hybrid Methods Engineering*, 2, pp. 233-247, 2000. (article)
- Boualit, A.**, Contribution à l'étude thermohydrodynamique des fluides Binghamien, Ph.D. thesis, University of Boumerdes, Algeria, 2011. (thesis)
- Johnston, P. R.**, Axial conduction and the graetz problem for a Bingham plastic in laminar tube flow. *International Journal of Heat and Mass Transfer*, 34, pp. 1209-1217, 1991. (article)
- Nouar, C.**, Thermal convection for a thermo-dependent yield stress fluid in an axisymmetric horizontal duct. *International Journal of Heat and Mass Transfer*, 48, pp. 5520-5535, 2005. (article)
- Soares, E. J., Naccache, M. F., and Mendes, P. R. S.**, Heat transfer to viscoplastic materials flowing axially through concentric annuli, *International Journal of Heat and Fluid Flow*, 24, pp. 762-773, 2003. (article)
- Sefid, M. M., and Izadpanah, E.**, Developing and Fully Developed Non-Newtonian Fluid Flow and Heat Transfer Through Concentric Annuli, *Journal of Heat Transfer*, 135, pp. 1-8, 2013. (article)
- Monteiro, E. R., Macêdo, E. N., Quaresma, J. N. N., and Cotta, R. M.**, Laminar flow and convective heat transfer of non-Newtonian fluids in doubly connected ducts. *International Journal of Heat and Mass Transfer*, 53, pp. 2434-2448, 2010. (article)
- Nouar, C., and Lebouche, M.**, Thermal convection for a thermodependent Herschel-Bulkley fluid in an annular duct. *Heat and Mass Transfer*, 31, pp. 257-267, 1996. (article)
- Nouar, C., Benaouda-Zouaoui, B., and Desaubry, C.**, Laminar mixed convection in a horizontal annular duct. Case of thermodependent non-Newtonian fluid. *European Journal of Mechanics B-Fluids*, 12, pp. 423-452, 2000. (article)
- Ait-Messaoudene, N., Horimek, A., Nouar, C., and Benaouda-Zouaoui, B.**, Laminar mixed convection in an eccentric annular horizontal duct for a thermodependent non-Newtonian fluid, *International Journal of Heat and Mass Transfer*, 54, pp. 4220-4234, 2011. (article)
- Nouar, C., Devienne, R. and Lebouche, M.**, Convection thermique pour un fluide de Herschel-Bulkley dans la région d'entrée d'une conduite, *International Journal of Heat and Mass Transfer*, vol. 37, no. 1, pp. 1-12, 1994. (article)

Gratão, A. C. A., Silveira, V. Jr., and Telis-Romero, J., Laminar forced convection to a pseudoplastic fluid food in circular and annular ducts, *International Communication in Heat and Mass Transfer*, 33, pp. 451-457, 2006. (article)

Gratão, A. C. A., Silveira V. Jr., and Telis-Romero J., Laminar flow of soursop juice through concentric annuli: Friction factors and rheology, *Journal of Food Engineering*, 78, pp. 1343-1354, 2007. (article)

Bernardi, M., Silveira, V. Jr., Telis, V. R. N., Gabas, A. L. and Telis-Romero, J., Forced convection to laminar flow of liquid egg yolk in circular and annular ducts, *Brazilian Journal of Chemical Engineering*, vol. 26, no. 2, pp. 287-298, 2009. (article)

Bird, R. B., Armstrong, R. C. and Hassenger, O., Dynamics of polymeric liquids, Vol.1: Fluid Mechanics, 2nd ed. , pp.181-183, John Wiley and Sons, New York, USA, 1987. (book)

Nouar, C., Convection thermique pour un fluide rhéofluidifiant. Cas de L'écoulement de Couette Poiseuille, Ph.D. thesis, I.N.P.L, Nancy, France, 1986. (thesis)

Bird, R. B., Stewart, W. E. and Lightfoot, E. N., Transport Phenomena, 2nd ed., pp.53-56, John Wiley and Sons, New York, USA, 2002. (book).

Ilicali, C., and Engez, S. T., Laminar flow of power law fluid foods in concentric annuli. *Journal of Food Engineering*, 30, pp. 255-262, 1996. (article)

Midoux, N., Mécanique et rhéologie des fluides en génie chimique, 2nd ed., pp.176-184, Tec et Doc, Paris, 1993. (book)

O'Donovan, E. V., and Tanner, R. I., Numerical study of the Bingham squeeze film problem, *Journal of Non-Newtonian Fluid Mechanics*, 15, pp. 75-83, 1984. (article)

Shah, R. K., and London, A. L., Laminar flow forced convection heat transfer and Flow friction in straight and curved ducts -A summary of analytical solutions-, Technical Report No.75, pp.23-47, Department of Mechanical Engineering, Stanford, California, USA, 1971. (book)

Lin, M.J., Wang and, Q.W., Tao, W.Q., Developing laminar flow and heat transfer in annular-sector ducts, *Heat Transfer Engineering*, 21, pp. 53-61, 2000. (article)

Terhmina, O., and Mojtabi, A., Ecoulements de convection forcée en régimes dynamique et thermique non établis dans un espace annulaire, *International Journal of Heat and Mass Transfer*, vol. 31, no. 3, pp. 583-590, 1988. (article)

Nomenclature

b : Experimental coefficient in consistency expression
 Cp: Specific heat (J .Kg-1.°C -1)
 Dh: Hydraulic diameter (m)
 K : Fluid consistency (Pa.sn)
 n : Shear-thinning index
 Nu : Nusselt number = $1/(\theta_i - \theta_m)$
 Pe : Péclet number = $\rho CP Ud Dh / \lambda$
 Pn : Pearson number = $b\Phi Dh / \lambda$
 Re : Reynolds number = $\rho Ud Dh / \mu_0$
 r : Radial position
 R1 : Inner cylinder radius (m)
 R2 : Outer cylinder radius (m)
 r1 : Radius ratio = $R1/R2$
 T : Temperature (°C)
 U : Dimensionless axial velocity
 Ud: Mean axial velocity (m.s-1)
 V: Dimensionless radial velocity
 z : Dimensionless axial coordinate
 Zth : Dimensionless thermal entry length

Greek symbols

ρ : Fluid density (Kg .m-3)
 λ : Thermal conductivity (W .m-1.°C -1)
 θ : Dimensionless temperature
 θ_m : Dimensionless bulk temperature
 Φ : Heat flux density (W.m-2)
 μ_a : Dimensionless Apparent viscosity
 μ_0 : Wall-shear viscosity at the entrance section
(Pa.s)

Subscript/Superscript

e : Inlet
fd : Fully developed
1,2 : Cylinders index, (1:inner, 2:outer)
* : Dimensional quantity